Utility of a hybrid approach to the hadronic vacuum polarisation contribution to the muon anomalous magnetic moment.

C. T. H. Davies,[1,*] A. S. Kronfeld,[2] G. P. Lepage,[3,†] C. McNeile,[4] and R. S. Van de Water[2]

[1]*SUPA, School of Physics and Astronomy, University of Glasgow, Glasgow, G12 8QQ, UK*
[2]*Fermi National Accelerator Laboratory, Batavia, Illinois 60510, USA*
[3]*Laboratory for Elementary-Particle Physics, Cornell University, Ithaca, New York 14853, USA*
[4]*Centre for Mathematical Sciences, University of Plymouth, PL4 8AA, UK*

(Dated: November 1, 2024)

An accurate calculation of the leading-order hadronic vacuum polarisation (LOHVP) contribution to the anomalous magnetic moment of the muon (a_μ) is key to determining whether a discrepancy, suggesting new physics, exists between the Standard Model and experimental results. This calculation can be expressed as an integral over Euclidean time of a current-current correlator $G(t)$, where $G(t)$ can be calculated using lattice QCD or, with dispersion relations, from experimental data for $e^+e^- \to$ hadrons. The BMW/DMZ collaboration recently presented a hybrid approach in which $G(t)$ is calculated using lattice QCD for most of the contributing t range, but using experimental data for the largest t (lowest energy) region. Here we study the advantages of varying the position $t = t_1$ separating lattice QCD from data-driven contributions. The total LOHVP contribution should be independent of t_1, providing both a test of the experimental input and the robustness of the hybrid approach. We use this criterion and a correlated fit to show that Fermilab/HPQCD/MILC lattice QCD results from 2019 strongly favour the CMD-3 cross-section data for $e^+e^- \to \pi^+\pi^-$ over a combination of earlier experimental results for this channel. Further, the resulting total LOHVP contribution obtained is consistent with the result obtained by BMW/DMZ, and supports the scenario in which there is no significant discrepancy between the experimental value for a_μ and that expected in the Standard Model. We then discuss how improved lattice results in this hybrid approach could provide a more accurate total LOHVP across a wider range of t_1 values with an uncertainty that is smaller than that from either lattice QCD or data-driven approaches on their own.

I. INTRODUCTION

As the muon spins its magnetic moment probes the vacuum, interacting with the sea of virtual particles there. These interactions are reflected in the quantity known as the anomalous magnetic moment of the muon, a_μ, recently measured to 0.21 parts per million by the Muon $g-2$ experiment at Fermilab [1]. A discrepancy between the experimental value for a_μ and that calculated in the Standard Model (SM) would indicate the existence of new particles in the virtual sea, beyond those known in the SM. Indeed, such a discrepancy (of size $25(5) \times 10^{-10}$) does exist between the current experimental result and that given in the 2020 Theory White Paper (WP20) [2], with the experimental result being significantly higher. Since 2020, however, it has become clear that the contribution from interactions involving quarks and gluons needs more work. Specifically, the value quoted in WP20 for the largest such contribution, known as the leading-order hadronic vacuum polarisation contribution (LOHVP), has been called into question following several recent developments [3]. This makes it important to reassess how the LOHVP is determined, finding ways to maximise the information that is included and embed physical tests of the result where possible.

The LOHVP can be calculated in two different ways that will be discussed further below: the 'data-driven approach' and that using lattice QCD calculations. The LOHVP value quoted in WP20 came from the data-driven approach, using experimental results for the cross-section for e^+e^- annihilation to hadrons as a function of centre-of-mass energy. Using analyticity and the optical theorem, $a_\mu^{\rm LOHVP}$ is determined as an integral over the cross-section multiplied by a QED kernel function that emphasises low values of $\sqrt{s}$. The WP20 result of $693.1(4.0) \times 10^{-10}$ [2, 4–9] has been assigned a 0.6% uncertainty that allows for the tension between some of the experimental results available at that time, particularly those seen in the $e^+e^- \to \pi^+\pi^-$ channel around the ρ resonance which provides the dominant contribution to $a_\mu^{\rm LOHVP}$ [10–20]. In 2023 a new experimental determination of the $e^+e^- \to \pi^+\pi^-$ cross-section by the CMD-3 collaboration [21, 22] gave a result which is larger than previous values. The impact of this CMD-3 result on the combination of experimental results is yet to be fully assessed. Substituting the CMD-3 2π cross-section results for the average of other experimental values in the LOHVP, however, closes the gap between the experimental determination of a_μ and that expected in the SM [23].

Lattice QCD calculations of the LOHVP can be expressed as an integral over Euclidean time of a correlation function $G(t)$ between two electromagnetic currents. The lattice results for the LOHVP [24–32] at the time of WP20 gave an average of $711.6(18.4) \times 10^{-10}$, with a much larger (2.6%) uncertainty than the data-driven value. Key problems for the lattice QCD calculations are the degradation of the signal-to-noise ratio in $G(t)$ at large Euclidean times and the determination of finite-volume effects. The large uncertainty meant that the lattice average could not discriminate between the possible scenarios of 'no new physics' in a_μ versus 'possible new physics' as favoured by the WP20 data-driven LOHVP. The

* christine.davies@glasgow.ac.uk
† g.p.lepage@cornell.edu

first subpercent accurate lattice QCD result, by the BMW collaboration [33], was published too late to be included in the WP20 lattice average. The BMW value of $707.5(5.5) \times 10^{-10}$ for the LOHVP has a 0.8% uncertainty and is 2.1σ higher than the WP20 data-driven value.

The BMW collaboration found [33] that the significance of the tension between the lattice and data-driven results [9] was increased (to 3.7σ) by considering a partial LOHVP calculation in which the integral over Euclidean time is restricted to a 'time-window' (with rounded edges). This had been suggested earlier [26, 34] as a way to improve the accuracy of lattice QCD calculations by cutting out the noisy large time region. A more stringent comparison of values from different lattice groups using different discretisations of QCD is then possible and the 'intermediate window' between 0.4 fm and 1.0 fm was adopted for this comparison. There is now a striking agreement on the results for this time-window between multiple different lattice groups with uncertainties at the level of 1–2%. Given that results from six different quark formalisms have been used this constitutes one of the best tests of full lattice QCD that has been done. Results have been obtained for the connected light quark (u/d with $m_u = m_d$) contribution to this window [33, 35–42] and for the complete windowed contribution (including all flavours along with quark-line disconnected contributions and QED and $m_u \neq m_d$ corrections) [33, 38, 39, 41, 42].

The input cross-section data for the data-driven approach can be converted, via a Laplace transform, into a correlation function in Euclidean time [34] so that a direct comparison with lattice QCD for the time-windowed observables can be made. It is important to note that a disagreement for any time window is as serious as a disagreement for the complete LOHVP contribution and so it makes sense to perform the comparison where the lattice QCD results have comparable accuracy to those from the e^+e^- data. For the 0.4 – 1.0 fm intermediate time-window, individual lattice QCD results for the complete contribution report tensions between 3.6σ and 4.2σ with the value from the data-driven average corresponding to the experimental e^+e^- data used in WP20 [43]. The tension is even larger, exceeding 5σ for several lattice QCD calculations, if the connected light quark contribution to the window is considered alone [44]. This latter comparison requires analysis of specific hadronic channels in the e^+e^- data to separate out this single flavour contribution [45]. Reference [44] uses the KNT19 [9] compilation of experimental e^+e^- data and notes that the replacement in the KNT19 dataset of CMD-3 data for $e^+e^- \to \pi^+\pi^-$ [21] removes the discrepancy between lattice QCD and data-driven results for the connected light quark contribution to the intermediate time-window. This suggests that the lattice QCD results favour the CMD-3 data over earlier experimental measurements of the $e^+e^- \to \pi^+\pi^-$ cross-section.

Recently the BMW/DMZ collaboration [42] have determined a value for the LOHVP contribution using a hybrid technique [26, 34] in which the Euclidean time axis is divided in two and the result of a lattice QCD calculation from $t = 0$ up to 2.8 fm (giving 96% of the LOHVP value) is combined with a data-driven approach from 2.8 fm to $t = \infty$ (giving the remaining 4%). This reduces the statistical error from the lattice QCD calculation and the size (and hence uncertainty in) the finite-volume correction, both of which grow at large time. Further, the small size of the data-driven contribution means that even a sizeable relative error in this piece would have little impact. In fact BMW/DMZ stress that they see no tension in the e^+e^- experimental data in the t >2.8 fm region, because this is dominated by very low energies below the ρ meson peak. In this way BMW/DMZ aim to reduce the total uncertainty in the LOHVP over that from an equivalent pure lattice QCD result. Their value ($714.1(3.3) \times 10^{-10}$) has an uncertainty of 0.5%, to be compared with that from earlier lattice QCD calculations discussed above. The LOHVP value obtained by BMW/DMZ leads to the conclusion that the SM and experimental a_μ results are consistent with each other [1, 42]. Further lattice QCD calculations of comparable precision are needed, as well as resolutions to disagreements in the e^+e^- data, to confirm or refute this conclusion.

To this end we explore more systematically here how to combine lattice QCD and data-driven contributions in an optimal way, modifying and extending a method used in [26]. Our method also allows us to test to what extent the input contributions are consistent with each other. This is equivalent to a comparison of lattice QCD and data-driven results but also leads to a value for the LOHVP contribution. The lattice QCD results that we use to test the approach come from [46], which used 2019 lattice-QCD data [29] from the Fermilab Lattice, HPQCD and MILC collaborations, and the compilation of e^+e^- data is based on that of KNT19 [9].

The layout of the paper is as follows: Section II A describes the hybrid approach of combining lattice QCD (subsection II B) and $R_{e^+e^-}$ (subsection II C) data, before giving the results in subsection II D; Section III gives our conclusions on the utility of this approach and suggestions for future work. Table II in subsection II C and Tables IV and V in Appendix A give the values from $R_{e^+e^-}$ needed for future lattice QCD applications of the hybrid approach that could improve uncertainties over the results presented here.

II. ANALYSIS AND RESULTS

A. Hybrid approach

The LOHVP contribution to a_μ can be calculated from the (Euclidean) correlator

$$G(t) \equiv \sum_{f,f'} Q_f Q_{f'} \sum_{\vec{x}} Z_V^2 \langle j_f^i(\vec{x},t) j_{f'}^i(0)\rangle \qquad (1)$$

where f, f' label quark flavors, Q_f is the quark's electric charge in units of the electron charge, and $j^i \equiv \overline{q}\gamma^i q$ is a spatial component of the quark vector current, with renormalization factor Z_V. Given this correlator, the LOHVP contribution is obtained from an integral of the form

$$a_\mu^{\rm LOHVP} = \left(\frac{\alpha}{\pi}\right)^2 \int_0^\infty dt\, G(t) K_G(t) \qquad (2)$$

where the kernel $K_G(t)$ vanishes as $t \to 0$; see reference [34] for details.

The correlator $G(t)$ is readily calculated directly using lattice QCD for t values less than 2–3 fm. Beyond that point, however, statistical errors tend to overwhelm the Monte Carlo in current analyses. The correlator can also be calculated from experimental data for e^+e^- annihilation into hadrons using [34]

$$G_R(t) = \frac{1}{12\pi^2} \int_0^\infty dE\, E^2\, R_{e^+e^-}(E)\, \mathrm{e}^{-Et}, \tag{3}$$

where $E = \sqrt{s}$ is the center-of-momentum energy and $R_{e^+e^-}$ is the hadronic cross section divided by the leading order cross section for $e^+e^- \to \mu^+\mu^-$. This suggests a hybrid approach where $G(t)$ is calculated using lattice QCD for small t values and $R_{e^+e^-}$ data for large ts [26].

To implement this strategy, we divide a_μ^{LOHVP} into two parts,

$$a_\mu^{\mathrm{LOHVP}} = a_\mu^{\mathrm{LOHVP}}(0, t_1) + a_\mu^{\mathrm{LOHVP}}(t_1, \infty), \tag{4}$$

using a window function

$$\Theta_{\Delta t}(t_1 - t) = 1 - \Theta_{\Delta t}(t - t_1) \tag{5}$$

$$\equiv \frac{1}{2}\left[1 - \tanh\left(\frac{t - t_1}{\Delta t}\right)\right], \tag{6}$$

which is a step function with a rounded edge of width Δt:

$$\Theta_{\Delta t}(t_1 - t) \to \begin{cases} 1 & \text{for } t_1 - t \gg \Delta t \\ 0 & \text{for } t - t_1 \gg \Delta t. \end{cases} \tag{7}$$

Here we set $\Delta t = 0.15$ fm, as in [46]. We calculate

$$a_\mu^{\mathrm{LOHVP}}(0, t_1) \equiv \left(\frac{\alpha}{\pi}\right)^2 \int_0^\infty dt\, G_{\mathrm{lat}}(t) K_G(t) \Theta_{\Delta t}(t_1 - t) \tag{8}$$

from lattice QCD data that comes predominantly from $t \le t_1$. Contributions from $t \ge t_1$ are calculated from $R_{e^+e^-}$ data:

$$a_\mu^{\mathrm{LOHVP}}(t_1, \infty) \equiv \left(\frac{\alpha}{\pi}\right)^2 \int_0^\infty dt\, G_R(t) K_G(t) \Theta_{\Delta t}(t - t_1). \tag{9}$$

Final results for the total a_μ^{LOHVP} should be independent of t_1 within errors, but the error will grow as t_1 increases towards 3 fm, because of statistical errors from lattice QCD.

As t_1 increases $a_\mu^{\mathrm{LOHVP}}(t_1, \infty)$ is dominated by low-energy contributions from $R_{e^+e^-}$. We can demonstrate this by calculating the energy $E_{\max}(t_1)$ such that the bulk of the contribution to $a_\mu^{\mathrm{LOHVP}}(t_1, \infty)$ comes from $R_{e^+e^-}$ data with $E \le E_{\max}(t_1)$. To be precise we define $E_{\max}$ so that:

$$a_\mu^{\mathrm{LOHVP}}(t_1, \infty) - a_\mu^{\mathrm{LOHVP}}(t_1, \infty)\big|_{E \le E_{\max}} = 10^{-10}, \tag{10}$$

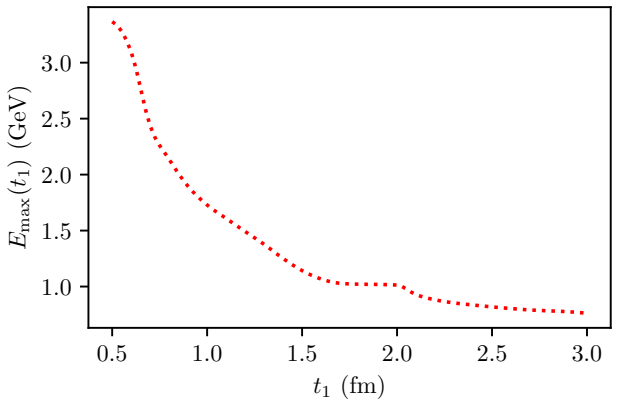

FIG. 1. $E_{\max}(t_1)$ as a function of t_1. The bulk of $a_\mu^{\mathrm{LOHVP}}(t_1, \infty)$ comes from $R_{e^+e^-}$ data with energy $E < E_{\max}(t_1)$. The shoulder around $E_{\max} = 1$ GeV is due to the strange quark threshold. There is a similar shoulder around 3 GeV from the charm threshold.

TABLE I. Lattice QCD results for $a_\mu^{\mathrm{LOHVP}}(0, t_1)$ from one-sided windows with various t_1 values [46]. The lattice results are added to results for $a_\mu^{\mathrm{LOHVP}}(t_1, \infty)$ obtained from the KNT19(CMD-3) [44] and KNT19 datasets [9] for $R_{e^+e^-}$ to obtain estimates for the full contribution a_μ^{LOHVP}. We denote the case with no lattice QCD contribution by setting t_1 to 'None';this is not the same as $t_1 = 0$ because of the windows rounded edges.

	$a_\mu^{\mathrm{LOHVP}}(0, t_1)$	a_μ^{LOHVP}	
t_1	LQCD	+ KNT19(CMD-3)	+ KNT19
None	0 (0)	714.7 (4.5)	692.7 (2.4)
0.5	99.9 (3)	715.2 (4.2)	694.4 (2.1)
1.0	304.0 (1.1)	714.0 (3.1)	698.8 (1.9)
1.5	495.5 (3.5)	711.6 (3.9)	703.2 (3.7)
2.0	605.0 (7.7)	705.3 (7.7)	701.4 (7.7)

where 10^{-10} is small compared with the current experimental uncertainty in a_μ (2.2×10^{-10} on the experimental average [1]). The value 10^{-10} is then a suitable tolerance to allow in the discussion of variations in the corresponding theoretical calculations. Figure 1 shows how $E_{\max}(t_1)$ falls from 3.4 GeV to 0.76 GeV as t_1 increases from 0.5 to 3.0 fm, respectively. By varying t_1 we probe the energy dependence of $R_{e^+e^-}$. Lattice QCD and $R_{e^+e^-}$ agree about that energy dependence insofar as results for the total a_μ^{LOHVP} are independent of t_1.

B. $a_\mu^{\mathrm{LOHVP}}(0, t_1)$ from lattice QCD

Table I lists results for $a_\mu^{\mathrm{LOHVP}}(0, t_1)$ taken from reference [46]. These are based on lattice QCD calculations, from 2019, by the Fermilab/HPQCD/MILC collaboration [29]. They use four sets of configurations with lattice spacings ranging from 0.15 to 0.06 fm, and $n_f = 2 + 1 + 1$ flavors of sea quarks. Note that the errors grow steadily as t_1 increases.

TABLE II. $a_\mu^{\rm LOHVP}(t_1,\infty)$ from KNT19(CMD-3) and KNT19 datasets for $R_{e^+e^-}$ for a range of t_1 values. Their difference is given in the final column. The fraction of the total $a_\mu^{\rm LOHVP}$ that comes from $a_\mu^{\rm LOHVP}(0,t_1)$ (i.e., from lattice QCD) is also listed for each t_1 value in the second column.

t_1	LQCD Frac.	KNT19(CMD-3)	KNT19	Diff.
None	0.000	714.7 (4.5)	692.7 (2.4)	21.9 (4.7)
0.4	0.097	645.6 (4.3)	624.3 (2.2)	21.3 (4.5)
0.5	0.139	615.3 (4.2)	594.5 (2.1)	20.8 (4.4)
1.0	0.426	410.0 (2.9)	394.8 (1.5)	15.2 (3.2)
1.5	0.698	216.1 (1.6)	207.7 (9)	8.3 (1.8)
1.9	0.835	117.6 (9)	113.0 (6)	4.6 (1.1)
2.0	0.860	100.3 (8)	96.4 (5)	3.9 (1.0)
2.5	0.937	44.9 (4)	43.2 (3)	1.7 (5)
2.8	0.961	27.8 (3)	26.8 (2)	1.0 (3)
3.0	0.972	20.4 (2)	19.6 (2)	0.7 (3)

C. $a_\mu^{\rm LOHVP}(t_1,\infty)$ from $R_{e^+e^-}$

Table II lists results for $a_\mu^{\rm LOHVP}(t_1,\infty)$ for a range of t_1 values. Results are given for two different datasets for $R_{e^+e^-}$. One uses the KNT19 dataset [9]. The other, KNT19(CMD-3), uses the same dataset but with the older $e^+e^- \to \pi^+\pi^-$ data replaced with data from CMD-3 [21]. For more details on this dataset see [44].

To obtain values for $a_\mu^{\rm LOHVP}(t_1,\infty)$, we used Eq. (3) to convert the $R_{e^+e^-}$ data into correlators $G_R(t)$ on a lattice with inverse lattice spacing $a^{-1} = 32\,$GeV, which corresponds to a lattice spacing a tenth the size of the smallest lattice spacing used in our simulations (so finite-a errors are negligible). Note that the uncertainties listed in Table II are highly correlated; see Appendix A.

The results for $a_\mu^{\rm LOVP}(t_1,\infty)$ from KNT19(CMD-3) and KNT19 datasets disagree by almost 5σ at small t_1. Figure 2 shows how this difference decreases with increasing t_1 until it is smaller than the experimental uncertainty in a_μ, for t_1 of order 2.5 fm and larger. Note that the difference is still significant (3σ) at $t_1 = 2.8$ fm (disagreeing with BMW/DMZ [42]), but is of small absolute size (1×10^{-10}) at that point because the contribution from $R_{e^+e^-}$ is so small. Figure 3 shows how the differences affect the Euclidean correlator $G_R(t)$, where the discrepancy is of order 4% for t between 2 and 3 fm. $\Delta G_R(t)$ falls to zero as $t \to 0$ because higher energy data (common to both datasets) then dominate Eq. (3).

D. Results

In Table I we combine results for $a_\mu^{\rm LOHVP}(0,t_1)$ from lattice QCD with results for $a_\mu^{\rm LOHVP}(t_1,\infty)$ from $R_{e^+e^-}$ to obtain estimates for the total $a_\mu^{\rm LOHVP}$. We do this using each of the KNT19(CMD-3) and KNT19 datasets for $R_{e^+e^-}$. Again the results from the different datasets do not agree, as is clear when they are plotted as a function of t_1 in Figure 4.

While the results must agree when extrapolated to large t_1, only the results from the newer KNT19(CMD-3) are independent of t_1 to within errors. We test the t_1 independence of the KNT19(CMD-3) results (blue circles) by fitting them to a constant, taking into account the strong correlations between the points at different t_1 values. This gives the weighted average of the five estimates of $a_\mu^{\rm LOHVP}$:

$$a_\mu^{\rm LOHVP}\big[\text{LQCD + KNT19(CMD-3)}\big] = 713.3(2.7)\times10^{-10} \tag{11}$$

with $\chi^2/{\rm dof} = 0.68$ for ${\rm dof} = 4$ degrees of freedom (p value 0.6). This is an excellent fit, unlike what happens when fitting the KTNT19 results (red diamonds):

$$a_\mu^{\rm LOHVP}\big[\text{LQCD + KNT19}\big] = 698.6(1.8)\times10^{-10} \tag{12}$$

with $\chi^2/{\rm dof} = 3.8$ for ${\rm dof} = 4$ degrees of freedom (p value 0.005). It is essential in these fits to account for the correlations.

Focusing on the results from lattice QCD combined with the KNT19 dataset, the increase in $a_\mu^{\rm LOHVP}$ as t_1 increases is

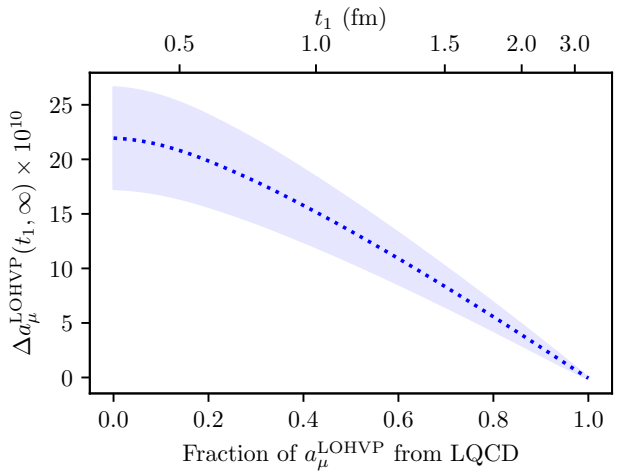

FIG. 2. Difference between estimates for $a_\mu^{\rm LOHVP}(t_1,\infty)$ made with the KNT19(CMD-3) and KNT19 data sets for $R_{e^+e^-}$. See Table II for details.

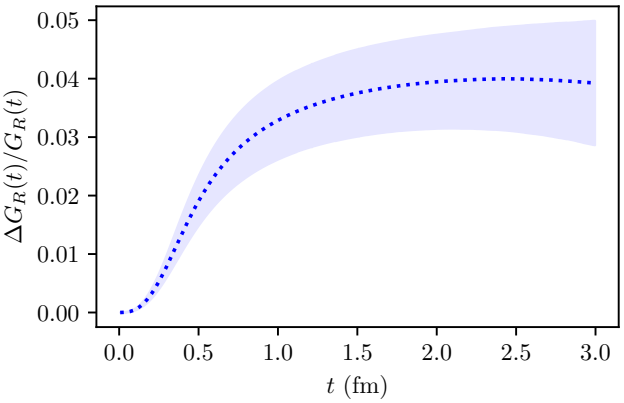

FIG. 3. Difference $\Delta G_R(t)$ between correlators $G_R(t)$ calculated with the KNT19(CMD-3) and KNT19 datasets, divided by $G_R(t)$ calculated with the KNT19(CMD-3) dataset.

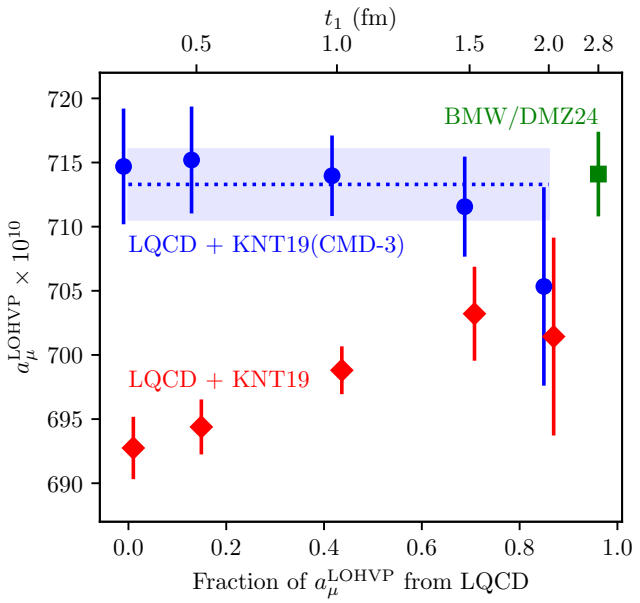

FIG. 4. Results for $a_\mu^{\rm LOHVP}$ from the hybrid approach plotted versus t_1. Results are given for two analyses, one that uses the KNT19(CMD-3) dataset for $R_{e^+e^-}$ (blue circles), and the other that uses the older KNT19 dataset (red diamonds). The recent result from BMW/DMZ [42] is also shown (green square).

TABLE III. Error budget showing % uncertainties in $a_\mu^{\rm LOHVP}$ calculated using the hybrid approach and the KNT19(CMD-3) dataset for $R_{e^+e^-}$. The uncertainties are given for different values of t_1 and for the weighted average of the results from different t_1s. The uncertainties come from: the KNT19 dataset for $R_{e^+e^-}$ with contributions from $e^+e^- \to \pi^+\pi^-$ removed; the contribution to $R_{e^+e^-}$ from CMD-3's results for $e^+e^- \to \pi^+\pi^-$; and lattice QCD.

t_1 (fm):	None	0.5	1.0	1.5	2.0	weighted avg.
$R_{e^+e^-}$(no $\pi\pi$):	0.21	0.15	0.08	0.04	0.01	0.08
$R_{e^+e^-}$(CMD-3 $\pi\pi$):	0.59	0.56	0.40	0.23	0.11	0.26
Lattice QCD:	0.00	0.04	0.15	0.50	1.09	0.27
Total:	0.63	0.58	0.44	0.55	1.10	0.38

roughly proportional to the fraction of $a_\mu^{\rm LOHVP}$ coming from lattice QCD. This suggests that the difference between the lattice results and those from the KNT19 data for $R_{e^+e^-}$ is an overall energy-independent multiplicative constant. We can make the KNT19 data consistent with the lattice results by multiplying the contributions to $R_{e^+e^-}$ from $e^+e^- \to \pi^+\pi^-$ by a factor of 1.0435. This gives a result that is very close to that from the KNT19(CMD-3) data (top panel in Figure 5), but with an uncertainty that is 30% smaller. Alternatively we can divide the lattice data by 1.022 (bottom panel of Figure 5) to obtain a result that is very close to what is obtained from the KNT19 dataset by itself, but with an uncertainty that is 25% smaller (if we average over all t_1). We provide Figure 5 to illustrate the issues arising from the difference between lattice QCD results and KNT19 $R_{e^+e^-}$ data and emphasise that neither of the factors used has any independent justification.

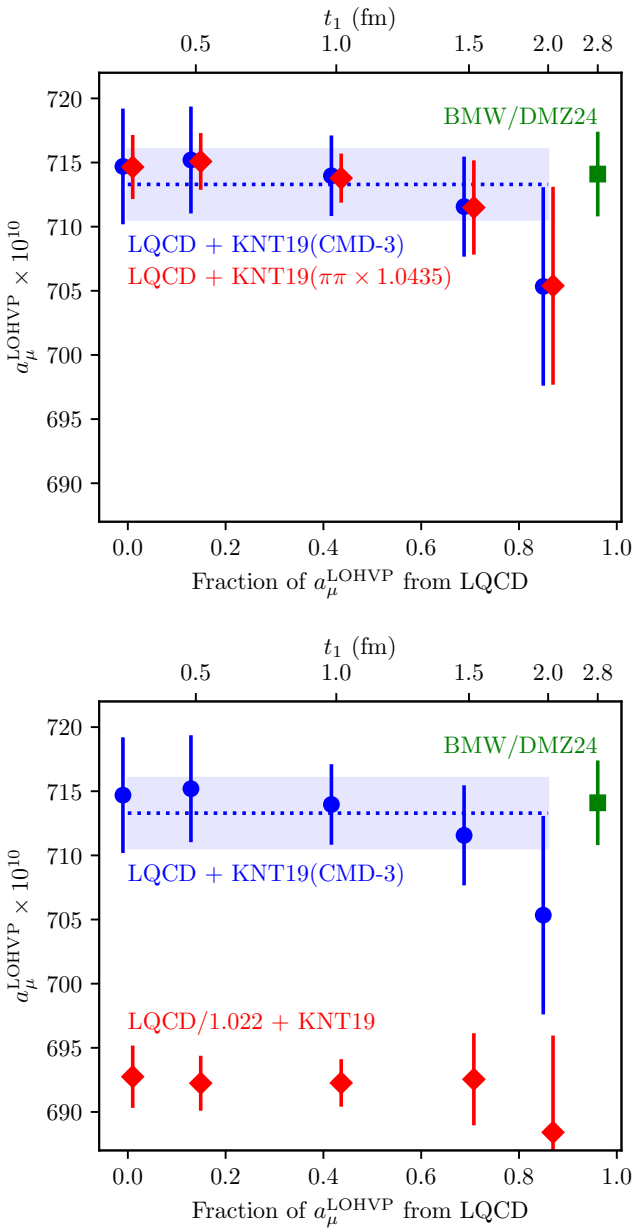

FIG. 5. Results for $a_\mu^{\rm LOHVP}$ from the lattice data combined with the KNT19 dataset (red diamonds) versus t_1 but with modifications to the $R_{e^+e^-}$ data (top panel) or the lattice results (bottom panel) that make the two consistent with each other. In the top panel, KNT19 results for $e^+e^- \to \pi^+\pi^-$ are multiplied by 1.0435. In the bottom panel the lattice results are divided by 1.022. Results based on the KNT19(CMD-3) dataset (blue circles) and from BMW/DMZ [42] (green square) are shown for comparison.

Lattice QCD strongly favors the KNT19(CMD-3) results over those from the KNT19 dataset. The KNT19(CMD-3) results also agree well with the recent result from BMW/DMZ [42] (green square in Figure 4), and are slightly more accurate when averaged.

Table III shows the error budget for $a_\mu^{\rm LOHVP}$ values obtained using the KNT19(CMD-3) dataset. As t_1 is increased,

the uncertainties decrease to a minimum around $t_1 = 1\,\text{fm}$. The most accurate estimate comes from the weighted average of the results from all t_1s, and its uncertainty is dominated equally by uncertainties from lattice QCD and from the CMD-3 results for $e^+e^- \to \pi^+\pi^-$.

III. CONCLUSIONS

The choice between a lattice QCD approach and a data-driven approach for calculating $a_\mu^{\rm LOHVP}$ is not binary. Rather these two approaches are the end-points for a continuum of possibilities labeled by t_1, the Euclidean time at which we switch from lattice data to $R_{e^+e^-}$ data when calculating the current-current correlator $G(t)$ from which $a_\mu^{\rm LOHVP}$ is determined.

There are two reasons for examining the entire t_1 dependence, and not just the endpoints or a fixed t_1 as in Ref. [42]. The first is to demonstrate that results are independent of t_1 within errors. When this is the case, it shows that lattice QCD and the $R_{e^+e^-}$ data agree on the energy dependence of $R_{e^+e^-}$. When this is not the case, there must be errors in either the lattice QCD analysis or the $R_{e^+e^-}$ data (or both). Our analysis shows that the KNT19 dataset for $R_{e^+e^-}$ is not consistent with the lattice QCD data of [46] because results are not independent of t_1. The t_1 region covered is one where lattice QCD calculations have proven to be reproducible[1]. Replacing the old data for $e^+e^- \to \pi^+\pi^-$ in the KNT19 dataset with the newer results from CMD-3 yields t_1 independence when combined with the lattice QCD data of [46]. These lattice QCD results thereby show a strong preference for the CMD-3 results over the older data. This agrees with the conclusions of the comparison of intermediate-distance time-windowed results between lattice QCD and e^+e^- data (see Section I for a discussion) but shows the effect more compellingly with multiple t_1 values.

The t_1 independence also strongly suggests that the pure lattice QCD result (in the $t_1 \to \infty$ limit) will agree with the purely data-driven result from KNT19(CMD-3). The larger the range of t_1 for which the combination of lattice QCD and $R_{e^+e^-}$ data remains flat the stronger that conclusion becomes as the contribution from the $R_{e^+e^-}$ data becomes smaller. Future lattice QCD calculations will be able to extend the range of t_1 values beyond those used here.

A second reason for examining the t_1 dependence is that the final uncertainty in $a_\mu^{\rm LOHVP}$ could well be smaller for intermediate values of t_1. This is the case for the KNT19(CMD-3) analysis we present here, where the uncertainty is smallest for $t_1 = 1\,\text{fm}$. It is smaller still when we calculate the weighted average of the results from different t_1s, giving us a value of $713.3(2.7) \times 10^{-10}$. This is significantly more accurate than the purely data-driven result for the KNT19(CMD-3) dataset in Table I. It is also slightly more accurate than the recent BMW/DMZ result of $714.1(3.3)\times10^{-10}$ [42], but agrees well with it and supports the conclusion that there is no significant discrepancy between the experimental results for a_μ and the Standard Model.

Much work is needed to come to a definitive answer on a_μ. It is imperative that the discrepancies between the CMD-3 and the older experimental $R_{e^+e^-}$ results be understood. Considering just the KNT19 data set, the discrepancy between lattice QCD and the $R_{e^+e^-}$ data suggests one of three possibilities: 1) there are 3–5% errors in the KNT19 data for $R_{e^+e^-}$ around 1 GeV or lower; 2) there are 3–5% errors in the eight lattice results at those energies; or 3) there is new physics, beyond the Standard Model, that affects $R_{e^+e^-}$ at the several percent level at those energies. The CMD-3 data set changes this discussion. If the old data in the KNT19 dataset are correct, then both the CMD-3 data set and the lattice QCD results must have errors at the 3–5% level. And those errors must conspire to make the hybrid $a_\mu^{\rm LOHVP}(t_1)$, calculated from CMD-3 data and lattice QCD results, independent of t_1 out to at least $t_1 = 1.5\,\text{fm}$. This would be surprising.

Without understanding the difference between CMD-3 and the older experimental $R_{e^+e^-}$ results one might conclude that a purely lattice QCD result for the LOHVP contribution is the only safe input for the Standard Model value for a_μ (unless you believe option 2 above, that there are unexplained errors in the lattice QCD results). It is still challenging for multiple lattice QCD groups to achieve $\sim 1\%$ uncertainties on the full LOHVP, however. Instead we argue that a combination of lattice QCD and data-driven results is a way forward. Accepting that lattice QCD is correct means that lattice QCD can be used to test the $R_{e^+e^-}$ results, as we have done here, and to select the option that is consistent with t_1 independence (if such an option exists). Alternatively it is possible to focus on a large enough value of t_1 that the data-driven contribution is small and the systematic error from differences between experiments is not unduly large. This latter approach is the one taken by BMW/DMZ with $t_1 = 2.8$ fm but, as we show in Table II, a smaller t_1 value of 2.5 fm or even 2.0 fm can be used without the differences between KNT19 and KNT19(CMD-3) exceeding 1% of the LOHVP contribution.

In this way, the uncertainty in the Standard Model prediction could be reduced in future with improved lattice QCD results for a wider range of t_1 values. In Table II we give the numbers for $a_\mu^{\rm LOHVP}(t_1,\infty)$ from $R_{e^+e^-}$ to be added to the lattice QCD results for a variety of t_1 values to obtain $a_\mu^{\rm LOHVP}$ and repeat the analysis done here. The correlation matrices for these numbers are given in Tables IV and V. The approach suggested here also provides a simple test of new experimental results for $R_{e^+e^-}$. Values for $a_\mu^{\rm LOHVP}(t_1,\infty)$ calculated from the new results can be combined with the lattice $a_\mu^{\rm LOHVP}(0,t_1)$ values given in Table I (with correlation matrix in Eq.(A1)), or improved lattice results when they become available. The lattice QCD results used here are from 2019 and more recent lattice data from, for example, Fermilab/HPQCD/MILC, has higher statistics and includes results on finer lattices [40]. From the error budget in Table III we see that halving the lattice QCD uncertainty at $t_1 =$ 2.0 fm would reduce the uncertainty on $a_\mu^{\rm LOHVP}$ to 0.56%

[1] See [46] for a comparison with other lattice QCD results in the 0.0–1.0 fm time-window.

using KNT19(CMD-3) results, or 0.8% if an additional uncertainty is allowed for the difference between KNT19 and KNT19(CMD-3). This is achievable in the near future.

Appendix A

The uncertainties in the lattice QCD results for $a_\mu^{\rm LOHVP}(0,t_1)$ in Table I are correlated. The correlation matrix for the results at $t_1 = 0.5$, 1.0, 1.5, and 2.0 fm is

$$\begin{pmatrix} 1.0000 & 0.3110 & 0.1840 & 0.1135 \\ 0.3110 & 1.0000 & 0.5484 & 0.4034 \\ 0.1840 & 0.5484 & 1.0000 & 0.7287 \\ 0.1135 & 0.4034 & 0.7287 & 1.0000 \end{pmatrix} \tag{A1}$$

Similarly the uncertainties in $a_\mu^{\rm LOHVP}(t_1,\infty)$ listed in Table II are (highly) correlated. The correlation matrices for the two datasets are given in Tables IV and V. There is no correlation between the lattice QCD and $R_{e^+e^-}$ results.

Acknowledgements

We are grateful to Alex Keshavarzi for providing the KNT19 and KNT19(CMD-3) datasets. In addition we are grateful to him and to Thomas Teubner for many useful discussions. The lattice QCD results used here come from [29]. We enjoyed stimulating discussions over these results with the co-authors of that work and are grateful for the collaboration. The lattice QCD results used the DiRAC Data Analytic system at the University of Cambridge, operated by the University of Cambridge High Performance Computing Service on behalf of the STFC DiRAC HPC Facility (www.dirac.ac.uk). This equipment was funded by BIS National E-infrastructure capital grant (ST/K001590/1), STFC capital grants ST/H008861/1 and ST/H00887X/1, and STFC DiRAC Operations grant ST/K00333X/1. DiRAC is part of the National E-Infrastructure. We are grateful to the Cambridge HPC support staff for assistance. Computations for the lattice QCD results were also carried out with resources provided by the USQCD Collaboration, the National Energy Research Scientific Computing Center and the Argonne Leadership Computing Facility, which are funded by the Office of Science of the U.S. Department of Energy. The lattice QCD work used the Extreme Science and Engineering Discovery Environment (XSEDE) supercomputer Stampede 2 at the Texas Advanced Computing Center (TACC) through allocation TG-MCA93S002. The XSEDE program is supported by the National Science Foundation under grant number ACI-1548562. Computations on the Big Red II+ supercomputer were supported in part by Lilly Endowment, Inc., through its support for the Indiana University Pervasive Technology Institute. The parallel file system employed by Big Red II+ is supported by the National Science Foundation under Grant No. CNS-0521433. The lattice QCD results also utilized the RMACC Summit supercomputer, which is supported by the National Science Foundation (awards ACI-1532235 and ACI-1532236), the University of Colorado Boulder, and Colorado State University. The Summit supercomputer is a joint effort of the University of Colorado Boulder and Colorado State University. Some of the computations were done using the Blue Waters sustained-petascale computer, which was supported by the National Science Foundation (awards OCI-0725070 and ACI-1238993) and the state of Illinois. Blue Waters was a joint effort of the University of Illinois at Urbana-Champaign and its National Center for Supercomputing Applications.

Funding for this work came from the Science and Technology Facilities Council and the National Science Foundation.

[1] D. P. Aguillard *et al.* (Muon $g-2$), Phys. Rev. Lett. **131**, 161802 (2023), arXiv:2308.06230 [hep-ex].

[2] T. Aoyama *et al.*, Phys. Rept. **887**, 1 (2020), arXiv:2006.04822 [hep-ph].

[3] "The status of Muon $g-2$ Theory in the Standard Model," (August 2023), Muon $g-2$ Theory Initiative, https://muon-gm2-theory.illinois.edu.

[4] M. Davier, A. Hoecker, B. Malaescu, and Z. Zhang, Eur. Phys. J. **C77**, 827 (2017), arXiv:1706.09436 [hep-ph].

[5] A. Keshavarzi, D. Nomura, and T. Teubner, Phys. Rev. **D97**, 114025 (2018), arXiv:1802.02995 [hep-ph].

[6] G. Colangelo, M. Hoferichter, and P. Stoffer, JHEP **02**, 006 (2019), arXiv:1810.00007 [hep-ph].

[7] M. Hoferichter, B.-L. Hoid, and B. Kubis, JHEP **08**, 137 (2019), arXiv:1907.01556 [hep-ph].

[8] M. Davier, A. Hoecker, B. Malaescu, and Z. Zhang, Eur. Phys. J. **C80**, 241 (2020), [Erratum: Eur. Phys. J. **C80**, 410 (2020)], arXiv:1908.00921 [hep-ph].

[9] A. Keshavarzi, D. Nomura, and T. Teubner, Phys. Rev. **D101**, 014029 (2020), arXiv:1911.00367 [hep-ph].

[10] R. R. Akhmetshin *et al.* (CMD-2), Phys. Lett. **B578**, 285 (2004), arXiv:hep-ex/0308008 [hep-ex].

[11] V. M. Aul'chenko *et al.* (CMD-2), JETP Lett. **82**, 743 (2005), [Pisma Zh. Eksp. Teor. Fiz. **82**, 841 (2005)], arXiv:hep-ex/0603021 [hep-ex].

[12] V. M. Aul'chenko *et al.* (CMD-2), JETP Lett. **84**, 413 (2006), [Pisma Zh. Eksp. Teor. Fiz. **84**, 491 (2006)], arXiv:hep-ex/0610016 [hep-ex].

[13] R. R. Akhmetshin *et al.* (CMD-2), Phys. Lett. **B648**, 28 (2007), arXiv:hep-ex/0610021 [hep-ex].

[14] M. N. Achasov *et al.* (SND), J. Exp. Theor. Phys. **103**, 380 (2006), [Zh. Eksp. Teor. Fiz. **130**, 437 (2006)], arXiv:hep-ex/0605013 [hep-ex].

[15] F. Ambrosino *et al.* (KLOE), Phys. Lett. **B670**, 285 (2009), arXiv:0809.3950 [hep-ex].

[16] F. Ambrosino *et al.* (KLOE), Phys. Lett. **B700**, 102 (2011), arXiv:1006.5313 [hep-ex].

[17] D. Babusci *et al.* (KLOE), Phys. Lett. **B720**, 336 (2013), arXiv:1212.4524 [hep-ex].

[18] A. Anastasi *et al.* (KLOE-2), JHEP **03**, 173 (2018),

TABLE IV. Correlation matrix for KNT19(CMD-3) results in Table II.

t_1	None	0.4	0.5	1.0	1.5	1.9	2.0	2.5	2.8	3.0
None	1.0000	0.9949	0.9915	0.9748	0.9588	0.9371	0.9295	0.8758	0.8331	0.8019
0.4	0.9949	1.0000	0.9995	0.9900	0.9758	0.9544	0.9468	0.8927	0.8496	0.8180
0.5	0.9915	0.9995	1.0000	0.9935	0.9804	0.9595	0.9520	0.8982	0.8550	0.8234
1.0	0.9748	0.9900	0.9935	1.0000	0.9947	0.9789	0.9725	0.9241	0.8834	0.8528
1.5	0.9588	0.9758	0.9804	0.9947	1.0000	0.9942	0.9906	0.9551	0.9209	0.8936
1.9	0.9371	0.9544	0.9595	0.9789	0.9942	1.0000	0.9995	0.9807	0.9554	0.9328
2.0	0.9295	0.9468	0.9520	0.9725	0.9906	0.9995	1.0000	0.9861	0.9635	0.9426
2.5	0.8758	0.8927	0.8982	0.9241	0.9551	0.9807	0.9861	1.0000	0.9942	0.9834
2.8	0.8331	0.8496	0.8550	0.8834	0.9209	0.9554	0.9635	0.9942	1.0000	0.9971
3.0	0.8019	0.8180	0.8234	0.8528	0.8936	0.9328	0.9426	0.9834	0.9971	1.0000

TABLE V. Correlation matrix for KNT19 results in Table II.

t_1	None	0.4	0.5	1.0	1.5	1.9	2.0	2.5	2.8	3.0
None	1.0000	0.9827	0.9711	0.9053	0.8343	0.7585	0.7376	0.6361	0.5839	0.5536
0.4	0.9827	1.0000	0.9982	0.9576	0.8907	0.8129	0.7912	0.6846	0.6293	0.5972
0.5	0.9711	0.9982	1.0000	0.9714	0.9086	0.8317	0.8100	0.7027	0.6469	0.6143
1.0	0.9053	0.9576	0.9714	1.0000	0.9748	0.9175	0.8993	0.8034	0.7501	0.7180
1.5	0.8343	0.8907	0.9086	0.9748	1.0000	0.9820	0.9726	0.9093	0.8678	0.8410
1.9	0.7585	0.8129	0.8317	0.9175	0.9820	1.0000	0.9990	0.9704	0.9430	0.9234
2.0	0.7376	0.7912	0.8100	0.8993	0.9726	0.9990	1.0000	0.9802	0.9567	0.9391
2.5	0.6361	0.6846	0.7027	0.8034	0.9093	0.9704	0.9802	1.0000	0.9951	0.9878
2.8	0.5839	0.6293	0.6469	0.7501	0.8678	0.9430	0.9567	0.9951	1.0000	0.9983
3.0	0.5536	0.5972	0.6143	0.7180	0.8410	0.9234	0.9391	0.9878	0.9983	1.0000

arXiv:1711.03085 [hep-ex].

[19] J. P. Lees *et al.* (BABAR), Phys. Rev. **D86**, 032013 (2012), arXiv:1205.2228 [hep-ex].

[20] M. Ablikim *et al.* (BESIII), Phys. Lett. **B753**, 629 (2016), arXiv:1507.08188 [hep-ex].

[21] F. V. Ignatov *et al.* (CMD-3), Phys. Rev. D **109**, 112002 (2024), arXiv:2302.08834 [hep-ex].

[22] F. V. Ignatov *et al.* (CMD-3), Phys. Rev. Lett. **132**, 231903 (2024), arXiv:2309.12910 [hep-ex].

[23] M. Davier, A. Hoecker, A.-M. Lutz, B. Malaescu, and Z. Zhang, Eur. Phys. J. C **84**, 721 (2024), arXiv:2312.02053 [hep-ph].

[24] B. Chakraborty *et al.* (Fermilab Lattice, HPQCD, MILC), Phys. Rev. Lett. **120**, 152001 (2018), arXiv:1710.11212 [hep-lat].

[25] S. Borsanyi *et al.* (Budapest-Marseille-Wuppertal), Phys. Rev. Lett. **121**, 022002 (2018), arXiv:1711.04980 [hep-lat].

[26] T. Blum, P. A. Boyle, V. Gülpers, T. Izubuchi, L. Jin, C. Jung, A. Jüttner, C. Lehner, A. Portelli, and J. T. Tsang (RBC, UKQCD), Phys. Rev. Lett. **121**, 022003 (2018), arXiv:1801.07224 [hep-lat].

[27] D. Giusti, V. Lubicz, G. Martinelli, F. Sanfilippo, and S. Simula, Phys. Rev. D **99**, 114502 (2019), arXiv:1901.10462 [hep-lat].

[28] E. Shintani and Y. Kuramashi (PACS), Phys. Rev. D **100**, 034517 (2019), arXiv:1902.00885 [hep-lat].

[29] C. T. H. Davies *et al.* (Fermilab Lattice, HPQCD, MILC), Phys. Rev. D **101**, 034512 (2020), arXiv:1902.04223 [hep-lat].

[30] A. Gérardin, M. Cè, G. von Hippel, B. Hörz, H. B. Meyer, D. Mohler, K. Ottnad, J. Wilhelm, and H. Wittig, Phys. Rev. D **100**, 014510 (2019), arXiv:1904.03120 [hep-lat].

[31] C. Aubin, T. Blum, C. Tu, M. Golterman, C. Jung, and S. Peris, Phys. Rev. D **101**, 014503 (2020), arXiv:1905.09307 [hep-lat].

[32] D. Giusti and S. Simula, PoS **LATTICE2019**, 104 (2019), arXiv:1910.03874 [hep-lat].

[33] S. Borsanyi *et al.*, Nature **593**, 51 (2021), arXiv:2002.12347 [hep-lat].

[34] D. Bernecker and H. B. Meyer, Eur. Phys. J. A **47**, 148 (2011), arXiv:1107.4388 [hep-lat].

[35] C. Lehner and A. S. Meyer, Phys. Rev. D **101**, 074515 (2020), arXiv:2003.04177 [hep-lat].

[36] G. Wang, T. Draper, K.-F. Liu, and Y.-B. Yang (χQCD), Phys. Rev. D **107**, 034513 (2023), arXiv:2204.01280 [hep-lat].

[37] C. Aubin, T. Blum, M. Golterman, and S. Peris, Phys. Rev. D **106**, 054503 (2022), arXiv:2204.12256 [hep-lat].

[38] M. Cè *et al.*, Phys. Rev. D **106**, 114502 (2022), arXiv:2206.06582 [hep-lat].

[39] C. Alexandrou *et al.* (Extended Twisted Mass), Phys. Rev. D **107**, 074506 (2023), arXiv:2206.15084 [hep-lat].

[40] A. Bazavov *et al.* (Fermilab Lattice, HPQCD, MILC), Phys. Rev. D **107**, 114514 (2023), arXiv:2301.08274 [hep-lat].

[41] T. Blum *et al.* (RBC, UKQCD), Phys. Rev. D **108**, 054507 (2023), arXiv:2301.08696 [hep-lat].

[42] A. Boccaletti *et al.*, (2024), arXiv:2407.10913 [hep-lat].

[43] G. Colangelo, A. X. El-Khadra, M. Hoferichter, A. Keshavarzi, C. Lehner, P. Stoffer, and T. Teubner, Phys. Lett. B **833**, 137313 (2022), arXiv:2205.12963 [hep-ph].

[44] G. Benton, D. Boito, M. Golterman, A. Keshavarzi, K. Maltman, and S. Peris, Phys. Rev. D **109**, 036010 (2024), arXiv:2311.09523 [hep-ph].

[45] G. Benton, D. Boito, M. Golterman, A. Keshavarzi, K. Maltman, and S. Peris, Phys. Rev. Lett. **131**, 251803 (2023), arXiv:2306.16808 [hep-ph].

[46] C. T. H. Davies *et al.* (Fermilab Lattice, MILC, HPQCD), Phys. Rev. D **106**, 074509 (2022), arXiv:2207.04765 [hep-lat].